

Accepted Manuscript

Title: Rhodium Nanoparticles Stabilized by Sulfonic Acid Functionalized Metal-Organic Framework for the Selective Hydrogenation of Phenol to Cyclohexanone

Author: Ahmet Bulut Mehmet Gulcan Ilknur Efecan Ertas
Mehmet Yurderi Mehmet Zahmakiran



PII: S1381-1169(15)30101-1
DOI: <http://dx.doi.org/doi:10.1016/j.molcata.2015.09.025>
Reference: MOLCAA 9641

To appear in: *Journal of Molecular Catalysis A: Chemical*

Received date: 18-5-2015
Revised date: 27-9-2015
Accepted date: 29-9-2015

Please cite this article as: Ahmet Bulut, Mehmet Gulcan, Ilknur Efecan Ertas, Mehmet Yurderi, Mehmet Zahmakiran, Rhodium Nanoparticles Stabilized by Sulfonic Acid Functionalized Metal-Organic Framework for the Selective Hydrogenation of Phenol to Cyclohexanone, *Journal of Molecular Catalysis A: Chemical* <http://dx.doi.org/10.1016/j.molcata.2015.09.025>

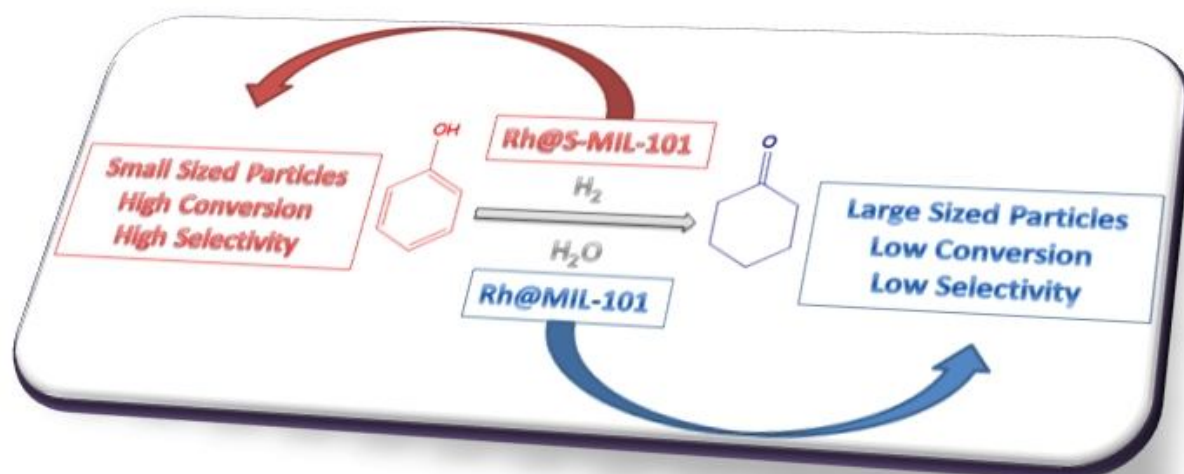
This is a PDF file of an unedited manuscript that has been accepted for publication. As a service to our customers we are providing this early version of the manuscript. The manuscript will undergo copyediting, typesetting, and review of the resulting proof before it is published in its final form. Please note that during the production process errors may be discovered which could affect the content, and all legal disclaimers that apply to the journal pertain.

Rhodium Nanoparticles Stabilized by Sulfonic Acid Functionalized Metal-Organic Framework for the Selective Hydrogenation of Phenol to Cyclohexanone

Ahmet Bulut,[†] Mehmet Gulcan,[†] Ilknur Efecan Ertas,[†] Mehmet Yurderi,[†] Mehmet Zahmakiran^{†,*}

[†] *Nanomaterials and Catalysis (NanoMatCat) Research Laboratory, Department of Chemistry, Yüzüncü Yıl University, 65080, Van, Turkey*

* Corresponding Author; e-mail: zmehmet@yyu.edu.tr; Fax: 90 432 225 18 06; Website: www.nanomatcat.com



Highlights:

- For the first time, Rh@S-MIL-101 catalyst was synthesized and characterized,
- For the first time, Rh@S-MIL-101 catalyst was used in phenol hydrogenation,
- Rh@S-MIL-101 provides remarkable catalytic performance in terms of activity, selectivity and reusability

Abstract

Rhodium(0) nanoparticles stabilized by sulfonic acid functionalized metal-organic framework (Rh@S-MIL-101) were prepared, for the first time, by using a direct cationic exchange approach and subsequent reduction with sodium borohydride at room temperature. The characterization of the resulting Rh@S-MIL-101 material was done by using multi pronged analyses including ICP-OES, EA, P-XRD, XPS, DR-UV-VIS, BFTEM, HRTEM, STEM-EDX and N₂-adsorption-desorption technique, which revealed that the formation of rhodium(0) nanoparticles (2.35 ± 0.9 nm) stabilized by the framework of S-MIL-101 by keeping the host framework intact (Rh@S-MIL-101). The catalytic performance of Rh@S-MIL-101 in terms of activity, selectivity and stability was demonstrated in the hydrogenation of phenol under mild conditions (at 50 °C and 5 bar initial H₂ pressure). We found that Rh@S-MIL-101 catalyst selectively hydrogenated phenol to cyclohexanone with high activity (*initial* TOF = 78 mol cyclohexanone/mol Rh×h) and selectivity (> 92 %) at almost complete conversion (> 95 %). Moreover, the resulting rhodium nanoparticles were found to be highly stable against leaching and sintering, which makes Rh@S-MIL-101 reusable heterogeneous catalyst without losing of significant activity and selectivity.

Keywords: Metal-Organic Framework; MIL-101; Rhodium; Phenol; Hydrogenation.

1. Introduction

In recent years, metal nanoparticles have been broadly explored in the search of enhanced catalytic performances as compared to their bulk-counterparts metal nanoparticles have much higher surface-to-volume ratio, thus, larger fraction of catalytically active atoms exist on their surface [1,2]. Because of high surface energies and large surface areas, metal nanoparticles are considered as thermodynamically unstable against to agglomeration into bulk form and therefore protecting ligands, polymers or capping agents must be used to stabilize them in their synthesis [3]. However, the aggregation of nanoparticles ultimately to the bulk metal despite using the best stabilizing agents [4,5] is still the most important problem that should be overcome in their catalytic applications. Additionally, it is another critical issue to obtain pure active metal surfaces by avoiding surface contamination from surface protecting groups, which often leads to a decrease in catalytic activities. In this context, the use of porous solid matrices as host material for guest metal nanoparticles immobilization allows the generation of specific surfactant-free active sites with the advantages of preventing particle aggregation [1-5].

In this context, porous materials like zeolites [6,7], carbonaceous materials [8,9], and minerals [10,11] have been widely used for fabricating metal nanoparticles within their porous matrices [12]. In addition to these porous materials, more recent studies [13-15] have also shown that metal-organic frameworks (MOFs), which are highly crystalline hybrid materials that combine metal ions with rigid organic ligands [16], can also be considered as suitable host materials to stabilize ligand-free guest metal nanoparticles. Indeed, MOFs can act as more suitable support material for metal nanoparticles with respect to other porous solids as they allow more flexible and systematic modification of the pore structure by the proper selection of the structural subunits and their connected ways [13-16]. Moreover, the stabilization of metal nanoparticles within the structure of MOFs can help us in the kinetic controlling of the catalytic reactions. The correct choosing of MOF's type under experimental conditions is the most critical step for the employment of MOFs as supports for metal nanoparticle immobilization as only a few MOFs with suitable pore structures are presently known for their thermal/chemical stability. The results of recent studies are showing that chromium(III) terephthalate framework; MIL-101 ($[\text{Cr}_3\text{F}(\text{H}_2\text{O})_2\text{O}\{\text{O}_2\text{CC}_6\text{H}_4(\text{CO}_2)\}_3.n\text{H}_2\text{O}]$; MIL:Materials Institut Lavoisier), which was first reported in 2005 by Ferey and co-workers [17], can be used in the stabilization of metal nanoparticles as it is stable in water even under very acidic conditions

and can show thermal stability up to 300 °C under air [18]. MIL-101 has very high surface area (~ 4100 m²/g) and contains two types of cages with diameters of 29 and 34 Å, which have pore apertures of 12 and 16 Å, respectively. These unique features of MIL-101 prompted us to focus on the use of the MIL-101 matrix in the stabilization of metal nanoparticles.

To date it has already been demonstrated that MIL-101 can act as a suitable host material for Pt [19], Pd [20-22], AuNi [23], AuPd [24], AgPd [25] and PdNi [26] nanoparticles. Xu et al. used “double-solvents” method to produce MIL-101 encapsulated Pt [19], AuNi [23], and AgPd [25] nanoparticles, which were found to be active catalysts in the hydrolysis of ammonia-borane [19,23] and one-pot cascade reactions [25]. Kempe and co-workers achieved the synthesis of bimetallic PdNi nanoparticles within the cavities of MIL-101 by gas phase infiltration of [(C₅H₅)Pd(C₃H₅)] and [(C₅H₅)₂Ni] followed by their dihydrogen reduction. The resulting PdNi@MIL-101 material acted as active catalyst in the reduction of 3-heptanone under mild conditions [26]. El-Shall et al. developed an effective microwave-assisted chemical reduction approach to incorporating Pd nanoparticles into MIL-101, and compared their activity toward CO oxidation of embedded Pd nanoparticles with those loaded on the outer surface [22]. Chang, Férey, and co-workers have realized more effective Pd encapsulation into MIL-101 by pre-grafting ethylenediamine (ED) on its coordinatively unsaturated Cr(III) centers. After treatment of the surface amine groups with an aqueous HCl solution, the positively charged ammonium groups undergo ionic reactions with anionic [PdCl₄]²⁻ salt by anionic exchange of the chloride anions and are finally reduced by sodium borohydride [20]. This methodology yields well-dispersed Pd nanoparticles stabilized by MIL-101 and they can act as active catalyst in the Heck type coupling reactions. Of particular importance, Zhu et. al. have recently reported that the preparation of sulfonic acid functionalized MIL-101 by the post-modification of the organic linkers under mild conditions [27]. The resulting sulfonic acid functionalized MIL-101 was found to be an efficient catalytic material that provides high conversions and activities in the esterification of monocarboxylic acids with monohydric alcohols. This study encouraged us to prepare MIL-101 confined metal nanoparticles in a new synthesis protocol that comprises of the neutralization of sulfonic acid with NaOH, then the ion-exchange between Na⁺ cations and Mⁿ⁺ cations followed by their borohydride reduction within the cages of MIL-101 under mild conditions.

Along this line, herein, we report the preparation and characterization of rhodium(0) nanoparticles stabilized by sulfonic acid functionalized MIL-101, hereafter referred to as Rh@S-MIL-101. As previously mentioned Rh@S-MIL-101 catalyst was reproducibly prepared by using a direct cationic exchange approach and subsequent reduction with sodium borohydride and characterized by inductively coupled plasma optical emission spectroscopy (ICP-OES), elemental analysis (EA), powder X-ray diffraction (P-XRD), X-ray photoelectron spectroscopy (XPS), diffuse reflectance UV-visible spectroscopy (DR-UV-VIS), bright-field transmission electron microscopy (BFTEM), scanning transmission electron microscope-energy dispersive X-ray spectroscopy (STEM-EDX), high resolution-TEM (HRTEM) and N₂-adsorption-desorption technique. The catalytic performance of these new rhodium(0) nanoparticles in terms of activity, selectivity and reusability was demonstrated in the aqueous phase phenol hydrogenation under mild reaction conditions.

2. Experimental

2.1. Materials

Chromium(III) nitrate nonahydrate (Cr(NO₃)₃·9H₂O), terephthalic acid (C₈H₆O₄), dimethylformamide (HCON(CH₃)₂), methanol (CH₃OH), acetone (CH₃COCH₃), trifluoromethanesulfonic acid (CF₃SO₃H), sulfuric acid (H₂SO₄), sodium borohydride (NaBH₄), rhodium(III) chloride trihydrate (RhCl₃·3H₂O), nitromethane (CH₃NO₂), phenol (C₆H₅OH), cyclohexanone (C₆H₁₀O), cyclohexanol (C₆H₁₁OH), ethanol (C₂H₅OH), dichloromethane (CH₂Cl₂), tetrahydrofuran (C₄H₈O), activated carbon (C), titanium(IV) oxide (TiO₂), nano-aluminum oxide (Al₂O₃) and silica (SiO₂) were purchased from Sigma-Aldrich. Deionized water was distilled by water purification system (Milli-Q Water Purification System). All glassware and Teflon coated magnetic stir bars were cleaned with acetone, followed by copious rinsing with distilled water before drying in an oven at 150 °C.

2.2. Characterization

The amount of rhodium loaded on S-MIL-101 and leached into the solution was determined by inductively couple plasma optical emission spectroscopy (ICP-OES) by using Perkin Elmer DRC II model (detection limit is 16 ppb for Rh). Elemental analyses were performed on LECO, CHNS-932 model. The powder X-ray diffraction (P-XRD) analyses were carried out on Rigaku Ultima-IV by using Cu-K α radiation (wavelength 1.54 Å, 40 kV, 55 mA). BFTEM and HRTEM

samples were prepared by dropping one drop of dilute suspension on copper coated carbon TEM grid and the solvent was then dried. BFTEM was carried out on a JEOL JEM-200CX transmission electron microscopes operating at 120 kV. HRTEM analyses were run on a JEOL JEM-2010F transmission electron microscope operating at 200 kV. The XPS analyses were performed on a Physical Electronics 5800 spectrometer equipped with a hemispherical analyzer and using monochromatic Al- K α radiation (1486.6 eV, the X-ray tube working at 15 kV and 350 W, and pass energy of 23.5 eV). DR-UV-VIS analyses were performed on Shimadzu UV-3600 modulated with integrating sphere attachment. The nitrogen adsorption-desorption experiment was carried out at 77 K using a NOVA3000 series instrument (Quantachrome Instruments). The sample was out-gassed under vacuum at 473 K for 3 h before the adsorption of nitrogen. The percent of exposed surface Rh atoms were obtained as 28, 38, 42, 34, 30 and 32 % of the total Rh atoms for Rh@S-MIL-101, Rh@MIL-101, Rh@C, Rh@SiO₂, Rh@TiO₂ and Rh@Al₂O₃ catalysts by CO chemisorption performed by Micromeritics 2010C instrument with the usual 1/1 (CO/Rh) stoichiometry [28].

2.3. Synthesis and Purification of MIL-101

MIL-101 was synthesized by following the slightly modified procedure given in the literature [29]. In a typical synthesis, Cr(NO₃)₃·9H₂O (2.0 g, 5 mmol), terephthalic acid (0.83 g, 5 mmol) and deionized water (20.0 mL) were mixed and homogenized by sonication at room temperature. Then, dark blue-colored suspension was placed in a Teflon-lined autoclave bomb and kept in oven at 220 °C. After the synthesis MIL-101 solids were separated from water using a centrifuge (5000 rpm, 10 min.) and washed with water, methanol and acetone. The final suspension in acetone was centrifuged and separated solid was placed in DMF (20.0 mL) and the suspension was sonicated for 10 min and kept at 70 °C for 12 h. The resulting solid powder was separated by centrifugation repeatedly washed with methanol and acetone, activated by drying at 150 °C for 12 h under vacuum (10⁻³ Torr). The yield of dried MIL-101 particles based on chromium was found to be 59 wt % and the typical EA and ICP-OES analyses: wt % C 47.0 and % Cr 9.8.

2.4. Sulfonic Acid Functionalization of MIL-101 (S-MIL-101)

Sulfonic acid functionalized MIL-101 was prepared by a post-modification method according to the procedure described in the literature [30]. 0.72 g activated MIL-101 was dispersed in 25.0 mL of nitromethane and then trifluoromethanesulfonic anhydride (1.5 mmol) and

concentrated sulphuric acid (1.0 mmol) were added into the suspension. Next, the mixture was continuously stirred in the water bath at room temperature for 1 h. The product was filtered and the solid was rinsed with deionized water and then with acetone, soaked in ethanol for 24 h at 70 °C, and dried in vacuum oven (10^{-1} Torr) at 150 °C for 6 h.

2.5. Synthesis of Sulfonic Acid Functionalized MIL-101 Stabilized Rhodium Nanoparticles (Rh@S-MIL-101)

The activated S-MIL-101 (190 mg) was treated with NaOH in 10.0 mL H₂O to pH = 9 and kept at this pH under vigorous agitation for 5 min. Then, filtered and dried host material was added into a solution of RhCl₃.3H₂O (20.3 mg ca., 5.0 wt % Rh) and this mixture was then stirred for other 6 h. Afterwards the reduction of Rh³⁺ was done by the addition of 1.0 mL aqueous sodium borohydride (110 mg; [NaBH₄]/[M] = 30) into the mixture kept in ice-bath. After 3 h the solid was centrifuged and washed with de-ionized water and ethanol and dried in vacuum oven (10^{-1} Torr) at 70 °C for 8 h. The rhodium content of the final material (Rh@S-MIL-101) was found to be 2.2 wt % by ICP-OES. Rh/S-MIL-101 catalyst was also prepared by following the similar synthesis protocol, which differs only in the reduction part. In this synthesis protocol Rh³⁺-exchanged S-MIL-101 was isolated by filtration, washed with excess water and dried in vacuum oven (10^{-1} Torr) at 70 °C for 4 h, and then reduced in 1.0 mL aqueous sodium borohydride solution (110 mg) kept in ice-bath. Afterwards the solid was centrifuged and washed with de-ionized water and ethanol and dried in vacuum oven (10^{-1} Torr) at 70 °C for 8 h. The rhodium content of Rh/S-MIL-101 was found to be 1.95 wt % by ICP-OES.

2.6. Synthesis of Rh@MIL-101, Rh@C, Rh@TiO₂, Rh@SiO₂ and Rh@Al₂O₃

In a four separate experiments 5.0 mL aqueous solution of RhCl₃.3H₂O (20.3 mg ca. 5.0 wt % Rh) was mixed with 190 mg support material (MIL-101, C, TiO₂, SiO₂ and Al₂O₃). Then, fresh 1.0 mL NaBH₄ (110 mg; [NaBH₄]/[M] = 30) solution in water was added separately to these mixtures and the resulting solutions were stirred for half an hour under air at room temperature. After centrifugation (6000 rpm, 5 min), copious washing with water (3 × 20 mL), filtration, and drying in oven at 100 °C, Rh@MIL-101, Rh@C, Rh@TiO₂, Rh@SiO₂ and Rh@Al₂O₃ catalysts were obtained as powders.

2.7. Catalytic Phenol Hydrogenation

The hydrogenation was carried out in a Teflon-lined stainless steel batch reactor (40 ml total volume) on the magnetic stirrer and this reactor was equipped with pressure transducer and transmitter that enabled us to monitor the pressure on the computer. In a typical experiment, phenol (235 mg, 2.5 mmol), catalyst (100 mg with 2.2 % wt Rh loading corresponds to 21.3 μmol Rh), and solvent (10.0 mL) were loaded into the reactor. The reactor was sealed and purged with H_2 to remove the air for 3 times, and then the reactor was heated to the desired temperature. The vapor pressure of solvent was released and hydrogen was introduced into the reactor after desired temperature was reached and the stirrer was started. After reaction the reactor was placed in ice water to quench the reaction and the products were analyzed on GC. All of the GC analyses were performed on a TRB-WAX column (30 m \times 0.25 mm \times 0.25 mm) with a Shimadzu GC-2010 equipped with a FID detector. The GC conditions for the product analysis were: injector port temperature: 250 $^\circ\text{C}$; column temperature: initial temperature: 50 $^\circ\text{C}$ (1 min); gradient rate: 20 $^\circ\text{C}/\text{min}$ (10 min); final temperature: 250 $^\circ\text{C}$ (3 min); flow rate: 80 ml/min. Cyclohexanone and cyclohexanol were the only reaction products observed. The selectivities and conversions were determined according to the literature methods [31].

2.8. Reusability Experiments

The reusability performance of Rh@S-MIL-101 was tested for phenol hydrogenation in water. The reaction was stopped after \sim 70 % conversion, the reaction mixture was centrifuged for 10 min and the liquid layer was siphoned out. The residual solid was washed with anhydrous ethanol and centrifuged twice and finally dried in a vacuum oven at 80 $^\circ\text{C}$ for 6 h. The catalyst was then weighed and reused under the same conditions.

3. Results and Discussion

Firstly, as-prepared Rh@S-MIL-101 was characterized by multi-pronged analyses including ICP-OES, EA, P-XRD, XPS, DR-UV-VIS, BFTEM, HRTEM, STEM-EDX and N_2 -adsorption-desorption technique. The EA and ICP-OES analyses revealed that the existence of S (0.26 wt %; 0.8 mmol/g; S/Cr = 0.87) and Rh (2.2 wt %; 0.21 mmol/g; S/Rh = 3.81) in the synthesized Rh@S-MIL-101. The sodium concentrations of S-MIL-101, Rh^{3+} @S-MIL-101 and Rh@S-MIL-101 were found to be 0.56, 0.25 and 0.41 mmol/g, respectively. The crystallinity of the host MIL-101 framework throughout the formation of both S-MIL-101 and Rh@S-MIL-101 was investigated by P-XRD (**Fig. 1**). The wide angle P-XRD patterns of S-MIL-101 and Rh@S-MIL-101 showed the

characteristic reflections of the host matrix MIL-101 [29], which confirmed the intact structure of MIL-101 after sulfonic acid functionalization and rhodium(0) nanoparticles formation.

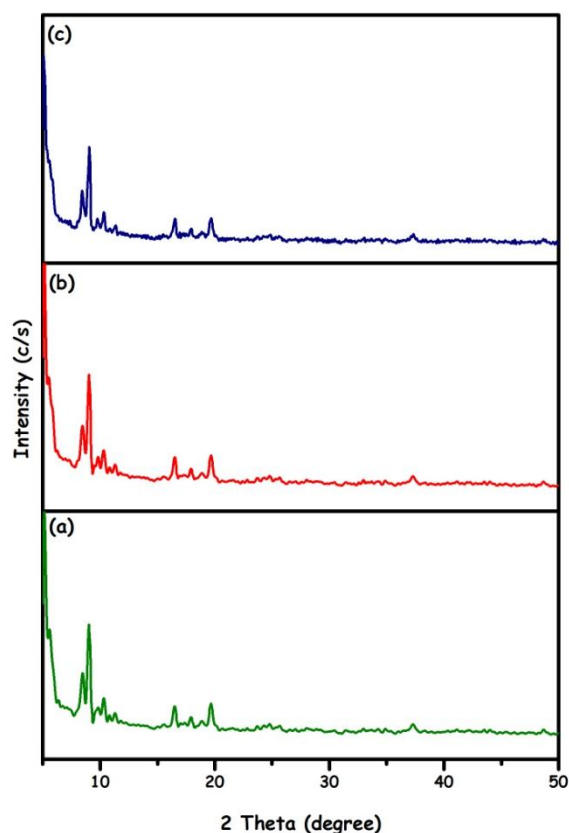


Fig. 1 Wide angle P-XRD patterns of (a) MIL-101, (b) S-MIL-101 and (c) Rh@S-MIL-101 (2.2 wt % Rh) in the range of $2\theta = 5-50^\circ$.

The decrease of the overall Bragg peaks intensity with respect to the parent, empty MIL-101 was a consequence of the inclusion of guest particles within the framework and has been well studied for zeolites and mesoporous silica materials [32,33]. In summary, the sum of P-XRD results is showing that neither the crystallinity nor the lattice of MIL-101 is distorted by formation of Rh nanoparticles within the sulfonic acid functionalized framework of MIL-101. **Fig. 2** shows DR-UV-VIS spectra of MIL-101, S-MIL-101 and Rh@S-MIL-101. The absorption bands observed at 451 and 600 nm in all of three MIL-101, S-MIL-101 and Rh@S-MIL-101 materials indicate that Cr (III) is present in distorted octahedral form [34]. After the sulfonic acid functionalization and rhodium incorporation, there was no distinguishable change observed in the DR-UV-VIS patterns, which is also indicative of host framework was reserved at the end of the synthesis of both S-MIL-101 and Rh@S-MIL-101.

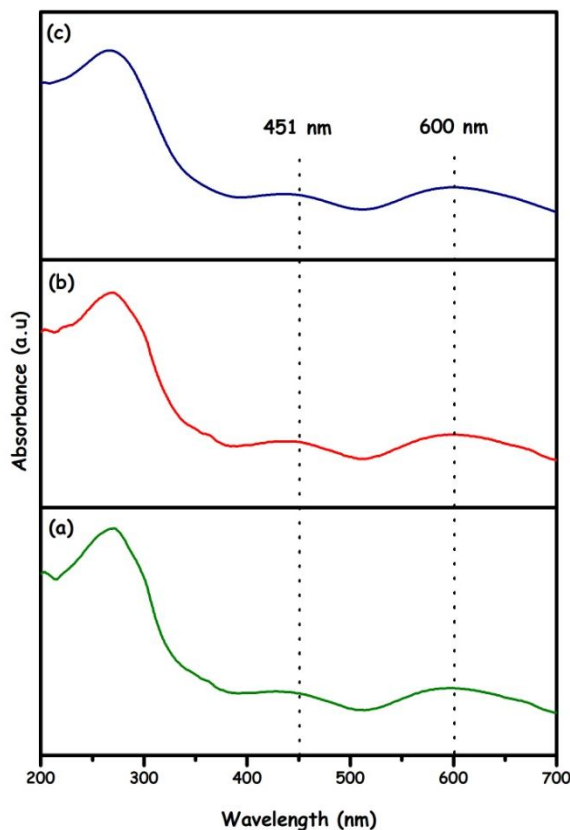


Fig. 2 DR-UV-VIS spectra of (a) MIL-101, (b) S-MIL-101 and (c) Rh@S-MIL-101 (2.2 wt % Rh) in the range of 200-700 nm.

The FTIR spectra of the synthesized MIL-101, S-MIL-101 and Rh@S-MIL-101 samples are compared in **Fig. 3**. For S-MIL-101 and Rh@S-MIL-101 new bands appeared at 1267, 1170, 1090, 1036 and 655 cm^{-1} . The bands observed at 1267 and 1170 cm^{-1} can be attributed to O=S=O symmetric and asymmetric stretching modes [27] and the peak at 1090 cm^{-1} is resulting from the S-O stretching vibration [27,35]. The peak at 655 cm^{-1} may be assigned to the C-S stretching vibration [31] and the additional peak at 1090 cm^{-1} corresponds to the skeletal vibration of the benzene rings substituted by a sulfonic acid group [27,35]. In the light of these and previously reported results [27, 36, 37] we can say that sulfonic acid groups are attached to the linker benzene rings in the framework of MIL-101.

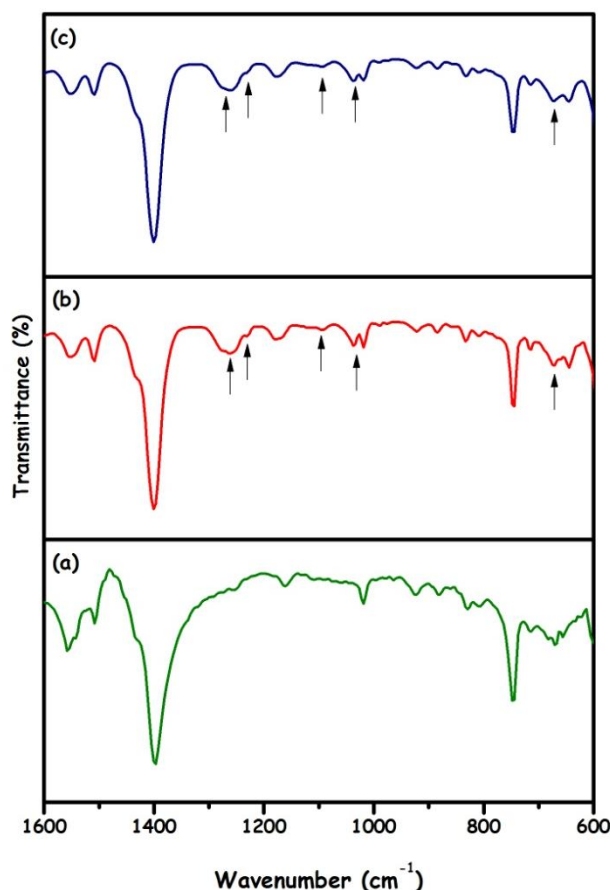


Fig. 3 FTIR spectra of (a) MIL-101, (b) S-MIL-101, (c) Rh@S-MIL-101 (2.2 wt % Rh) in the range of 1600-500 cm^{-1} .

Nitrogen adsorption-desorption isotherms of MIL-101, S-MIL-101 and Rh@S-MIL-101 are given in **Fig. 4** and all of them show type I shape, which is a characteristic for microporous materials [38]. The micropore volume and surface area were determined for MIL-101, S-MIL-101 and Rh@S-MIL-101 by the t -plot method [39]. On passing from MIL-101 \rightarrow S-MIL-101 \rightarrow Rh@S-MIL-101, both the micropore volume (from 1.59 cm^3/g \rightarrow 1.17 cm^3/g \rightarrow 1.01 cm^3/g) and BET surface area (from 3460 m^2/g \rightarrow 2640 m^2/g \rightarrow 2120 m^2/g) are noticeably reduced. The remarkable decrease in the micropore volume and surface area for S-MIL-101 and Rh@S-MIL-101 can be attributed to the encapsulation of bulky acid groups and rhodium nanoparticles in MIL-101. Furthermore, no hysteresis loop was observed in the N_2 adsorption-desorption isotherm of Rh@S-MIL-101, indicating that the procedure followed in the preparation of Rh@S-MIL-101 did not create any mesopores. XPS analysis was performed to investigate both the composition and the chemical state of the Rh@S-MIL-101.

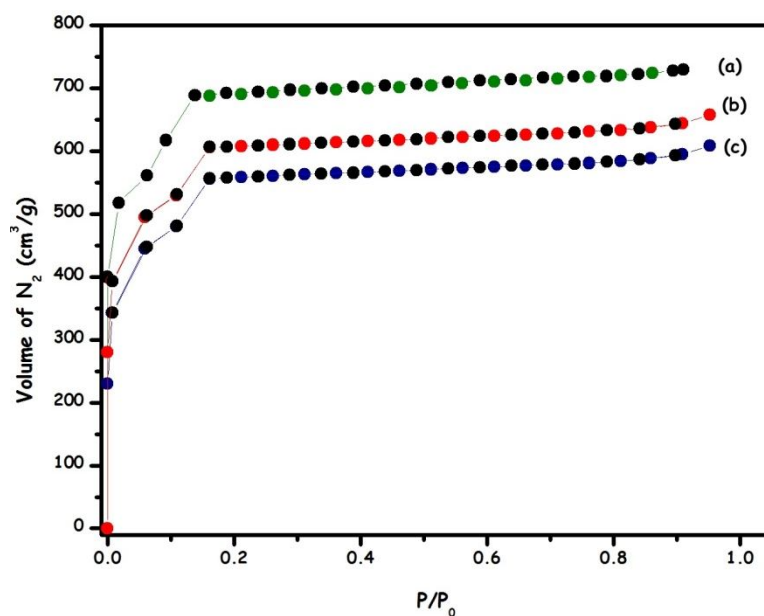


Fig. 4 N₂ adsorption-desorption isotherms of (a) MIL-101, (b) S-MIL-101 and (c) Rh@S-MIL-101 (2.2 wt % Rh).

Fig. 5 shows the wide-scan XPS spectrum of Rh@S-MIL-101, which revealed that the existence of Cr, S, Rh and Na elements. The main peaks were observed for rhodium at 497, 313.5 and 308.5 eV, which can readily be assigned to metallic Rh 3p_{3/2}, Rh 3d_{3/2} and Rh 3d_{5/2} [40,41].

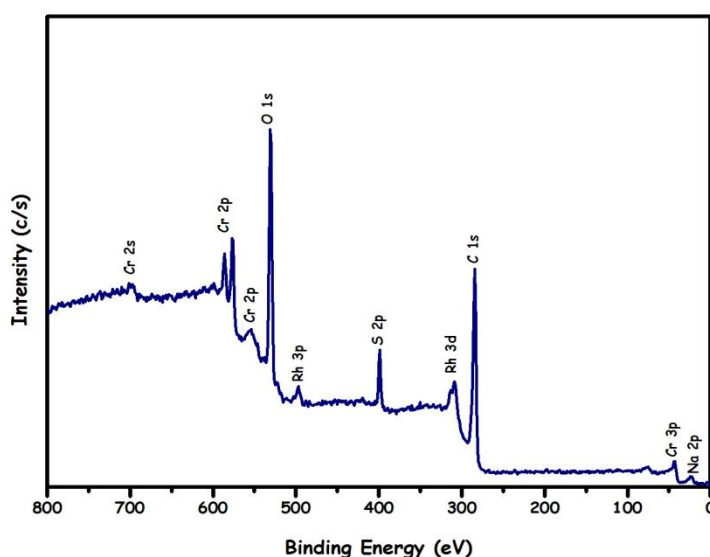


Fig. 5 The wide-scan XPS spectrum of Rh@S-MIL-101 (2.2 wt % Rh) in the range of 800-0 eV.

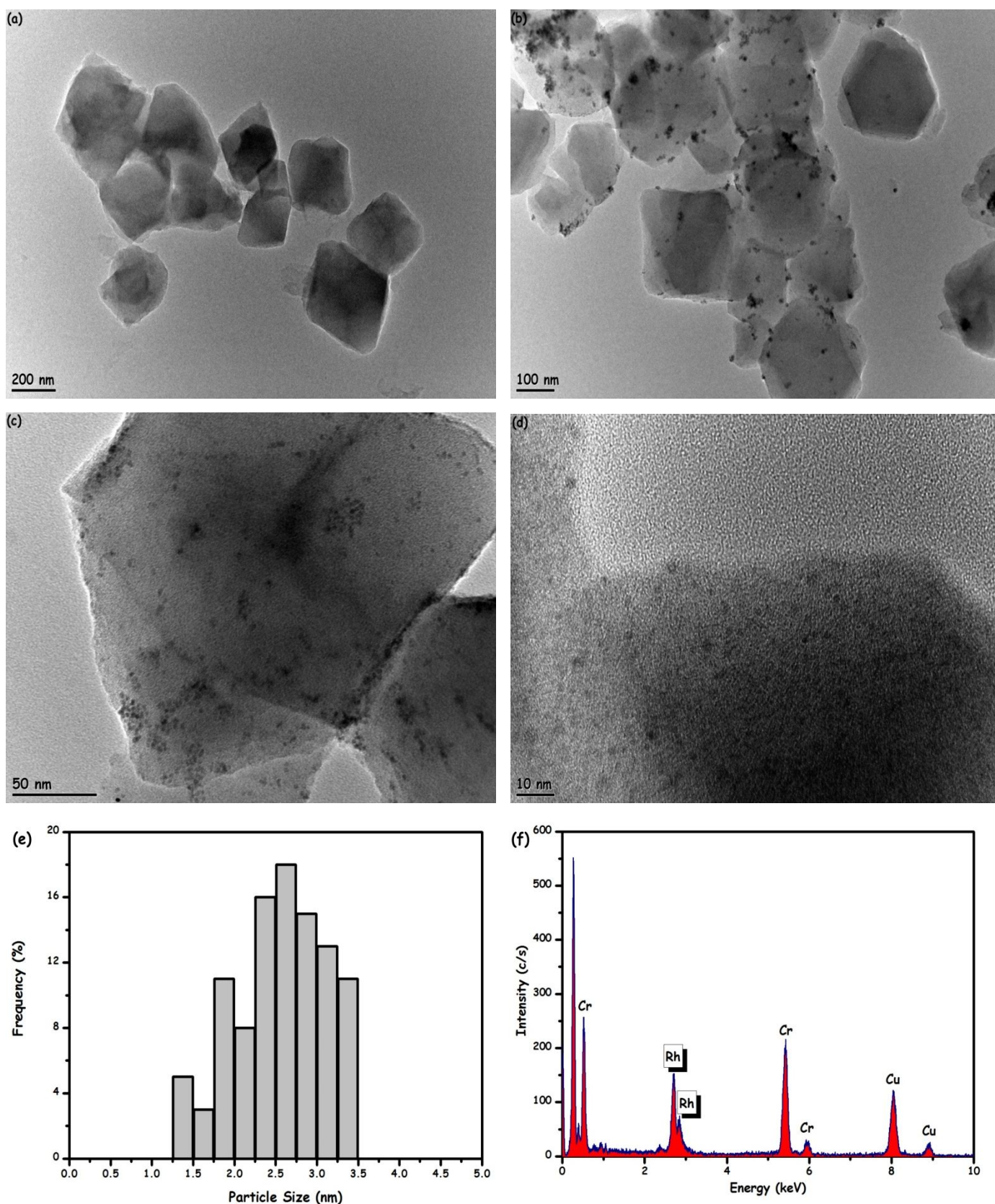


Fig. 6 (a) Low-resolution BFTEM image of Rh@S-MIL-101, (b) low-resolution BFTEM image of Rh@MIL-101, (c-d) BFTEM images of Rh@S-MIL-101 in different magnifications, (e) size histogram of Rh@S-MIL-101 and (f) STEM-EDX spectrum of Rh@S-MIL-101.

BFTEM, HRTEM, and STEM-EDX analyses were done to investigate the size, morphology and composition of Rh@S-MIL-101. The low resolution BFTEM image of Rh@S-MIL-101 (2.2 wt % Rh) given in **Fig. 6** (a) shows no bulk rhodium was formed on the surface of MIL-101 crystals. In contrast, much larger Rh agglomerates were obtained with unmodified MIL-101 sample that contained very close amount of Rh (2.1 wt % Rh) with that of Rh@S-MIL-101 (Fig. 6 (b)), which verified the effect of sulfonate to encapsulation and stabilization of metal nanoparticles. The conventional BFTEM images of Rh@S-MIL-101 in different magnifications (Figs. 6 (c-d)) showed that the presence of rhodium(0) nanoparticles in the range of 1.25 – 3.5 nm with a mean diameter of 2.35 ± 0.9 nm (Fig. 6 (e)). EDX spectrum collected during the STEM observation of Rh@S-MIL-101 from many different areas is given in Fig. 6 (f), which confirmed the presence of Rh in the analyzed region as judged by $L_{\alpha 1}$, $L_{\beta 1}$, $L_{\beta 1}$, and $L_{\beta 2}$ lines of rhodium in the range of 2.3–3.0 keV [42,43].

The catalytic performance of Rh@S-MIL-101 in terms of activity, selectivity and durability was investigated in the liquid phase hydrogenation of phenol, which offers cost and energy saving protocol for the production of industrially important cyclohexanone [44]. Many researchers have contributed to this area, and various heterogeneous catalysts have already been screened [31, 45-48]. However, the attainment of high selectivity (> 90 %) at elevated conversion (> 75 %) with a satisfactory rate is still a great challenge, because the cyclohexanone product can be further hydrogenated to cyclohexanol under the reaction conditions **(1)** [38]. Before testing the catalytic activity of Rh@S-MIL-101 in the phenol hydrogenation, one has to check whether the host material MIL-101, sulfonated MIL-101 (S-MIL-101) and Na^+ salt form of MIL-101 can catalyze this reaction under the same conditions. For this reason, the catalytic activities of these three Rh-free materials were investigated in the hydrogenation of phenol in water at 50 °C and 5 bar initial H_2 pressure. The result of these experiments showed that all of these materials were catalytically inactive in the hydrogenation of phenol. The activity of Rh@S-MIL-101 for the hydrogenation of phenol was then investigated. For our purpose, we first investigated the effect of various solvents and initial hydrogen pressure. The corresponding conversions and selectivities are listed in **Table 1**.

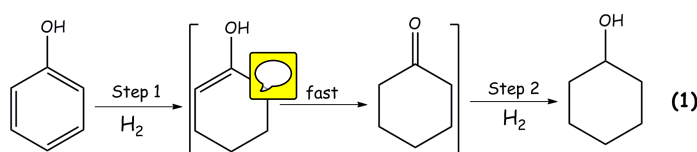


Table 1. The effect of reaction conditions on the conversion and selectivity of Rh@S-MIL-101 in the phenol hydrogenation.^a

Entry	Solvent	P _{H₂} (bar)	Conversion (%)	C=O Selectivity (%)	C-OH Selectivity (%)
1	H ₂ O	5	95	92	8
2	C ₄ H ₈ O (THF)	5	35	70	30
3	C ₂ H ₅ OH	5	80	65	35
4	CH ₂ Cl ₂	5	91	85	15
5	H ₂ O	7	99	82	18
6	H ₂ O	3	80	90	10
7	H ₂ O	1	60	89	11
8 ^b	H ₂ O	5	99	85	15
9 ^c	H ₂ O	5	55	82	18

^a In a typical reaction, 100 mg Rh@S-MIL-101 was used in the hydrogenation of 2.5 mmol phenol in 10 mL solvent at 50 °C. All conversion and selectivity values were determined at the end of 2 h; ^b Temperature was 100 °C and the reaction time was 1 h; ^c Temperature was 25 °C and the reaction time was 24 h.

With Rh@S-MIL-101 catalyst under reaction conditions, we could readily achieve selectivities toward cyclohexanone in the range of 65-92 % with a phenol conversion of 35-95 % in 2 h at 50 °C and 5 bar initial hydrogen pressure (entries 1-4 in Table 1). Among the tested solvents water exhibited the highest activity and selectivity values (entry 1). Dichloromethane (CH₂Cl₂) also gave high activity but with a low selectivity toward cyclohexanone (entry 4). We obtained the lowest conversion value with Rh@S-MIL-101 catalyst in THF (entry 2) as THF has positive acceptor number (δ) [49], which means that it is capable of transferring electrons to active Rh centers so deactivates Rh nanoparticles in phenol hydrogenation. Additionally, the lower activity of Rh@S-MIL-101 in ethanol (entry 3) with respect to water can be explained by the different solubility of phenol in water (8.3 g/100 mL) and ethanol (47 g/100 mL) [49]. Ethanol not only strongly solvates phenol and cyclohexanone but also adsorbs strongly on Rh. This strong adsorption of phenol/cyclohexanone reduces the phenol coverage on the Rh surface, affording slower phenol hydrogenation in ethanol. The variation in the reaction temperature and initial hydrogen pressure had considerable effects on the conversion and selectivity. Even at room temperature > 50 % conversion could be reached after a longer reaction time of 24 h (entry 9). The partial loss of the selectivity may be caused by the hydrogenation of cyclohexanone to cyclohexanol after a long reaction time, which could also be observed when

the temperature and initial hydrogen pressure were increased (entries 5 and 8). According to these results, we afterward limited the subsequent catalytic studies to aqueous phenol feed at 50 °C and 5 bar initial H₂ pressure. As can be seen from **Fig. 7**, Rh@S-MIL-101 (100 mg with 2.2 % wt Rh loading corresponds to 21.3 μmol Rh) showed very good activity (initial TOF = 78 mol cyclohexanone/mol Rh×h) and selectivity (> 90 %) throughout the course of the reaction (2.5 mmol phenol in 10.0 mL H₂O) at 50 °C (**2**). In order to find the true TOF value we also performed CO chemisorption analysis on Rh@S-MIL-101, which showed that ca. 28 % of total Rh metal atoms were exposed. Therefore the true TOF value was found to be Rh@S-MIL-101 is ~ 280 mol cyclohexanone/mol Rh×h by considering exposed surface Rh atoms.

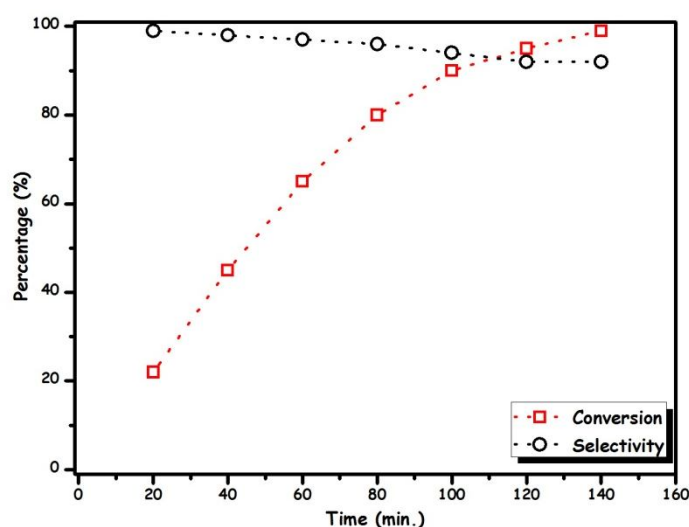
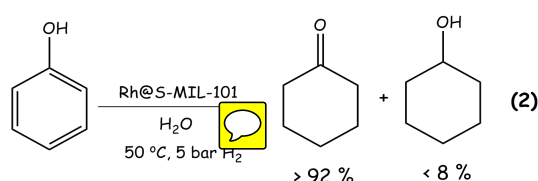


Fig. 7 The percentage of catalytic conversion and selectivity versus time graph for Rh@S-MIL-101 catalyzed phenol hydrogenation.

It is particularly remarkable that the selectivity values remain very close to 100 % until conversion values exceed 60 %, the final selectivity value > 92 % for > 98 % conversion was observed. The observed activity and selectivity values with Rh@S-MIL-101 are higher than those of previously reported rhodium based Rh/C (5.0 % wt Rh) [45] and Rh/C-nanofiber (5.0 % wt Rh) [46] catalysts, which can only work at harsh conditions (high temperature and initial H₂ pressure) and comparable with the previous best catalytic system for the hydrogenation of phenol to cyclohexanone (Pd@mpg-C₃N₄, TOF = 95 mol cyclohexanone/mol Pd×h) [47].



The uniqueness of Rh@S-MIL-101 was also compared with Rh@MIL-101 (2.1 wt % Rh), Rh@C (2.1 wt % Rh), Rh@TiO₂ (2.3 wt % Rh), Rh@SiO₂ (2.2 wt % Rh) and Rh@Al₂O₃ (2.3 wt % Rh) catalysts in the phenol hydrogenation under identical conditions. If the percentage of exposed surface Rh atoms was considered, the initial TOF values were found to be 118, 43, 93, 35 and 103 mol cyclohexanone/mol Rh×h for Rh@MIL-101, Rh@C, Rh@TiO₂, Rh@SiO₂ and Rh@Al₂O₃, respectively. The control experiments were also conducted to show that all of these metal-free support materials were catalytically inactive in phenol hydrogenation. Therefore the variation observed in the TOF values of these Rh-based heterogeneous catalysts can only be explained by considering the size/morphology of guest Rh nanoparticles and the nature of the support material (*vide infra*).

Table 2. The comparison of catalytic performances for the present Rh@S-MIL-101 with Rh based supported catalysts tested in this study.

Entry	Catalyst	Conversion (%)	C=O Selectivity (%)	C-OH Selectivity (%)
1	MIL-101	no activity	-	-
2	Rh@MIL-101	65	82	18
3	Rh@S-MIL-101	95	92	8
4	Rh@C	53	37	63
5	Rh@TiO ₂	54	63	37
6	Rh@SiO ₂	18	71	29
7	Rh@Al ₂ O ₃	54	72	28

^a In a typical reaction, 100 mg catalyst was used in the hydrogenation of 2.5 mmol phenol in 10 mL H₂O at 50 °C and 5 bar H₂. All conversion and selectivity values were determined at the end of 2 h.

The catalytic performances in terms of conversion and selectivity are also given in **Table 2**. As seen from Table 2 the best catalytic performance in terms of conversion and selectivity was achieved by Rh@S-MIL-101 catalyst. BFTEM analyses conducted on Rh@C, Rh@SiO₂, Rh@TiO₂ and Rh@Al₂O₃ (see **Fig. S1-S4** in the Supporting Information) catalysts showed that the formation of large size Rh(0) nanoparticles on the surface of these solid supports, which may indicate the confinement effect of sulfonated-MIL-101 (S-MIL-101) matrix to produce small sized Rh nanoparticles and explain the observation of lower activity and selectivity values with Rh@C, Rh@SiO₂, Rh@TiO₂ and Rh@Al₂O₃ catalysts. Additionally, the surface morphology of some of these (Rh@C and Rh@SiO₂) resulting Rh nanoparticles differed from Rh@S-MIL-101.

For example, highly clumped non-spherical Rh agglomerates formed on the surface of activated carbon and silica, which explains the observation of very low catalytic activities with Rh@C and Rh@SiO₂ catalysts. Although the formation of rhodium(0) agglomerates were also observed with unmodified MIL-101 (Fig. 6(b)), the enhanced selectivity of Rh@MIL-101 can be explained by the existence of Cr(III) Lewis acidic sites in MIL-101 framework, which inhibits further hydrogenation of cyclohexanone by interacting with Lewis basic C=O group [31].

In working with porous solid stabilized metal nanoparticles in heterogeneous catalysis, one of the most crucial questions is whether the nanoparticles in the cavities or on surface of solid support contribute more in catalysis. Performing of poisoning experiments by using large and small sized of N-, S- or P-bearing molecules is one of the well-known methodologies to investigate the distribution of these active metal nanoparticles [50, 51]. Unfortunately, it was difficult for us to perform these experiments in the case of using MIL-101 host framework, because its large size cavities (29 Å/ 34 Å) are not suitable to provide size selectivity to commonly used poisons such as P(C₆H₅)₃ [50, 51], CS₂ [52- 54] and 1,10-phenanthroline [55] as their kinetic diameters are smaller than the cage diameters of MIL-101, so they can poison both supported and confined nanoparticles. In this context, a control experiment was performed in which rhodium(0) nanoparticles stabilized by MIL-101 framework (hereafter referred to as Rh/S-MIL-101) was prepared under identical conditions given in the section of 2.5 except that only NaBH₄ reduction was conducted on the Rh³⁺-exchanged S-MIL-101 sample that was isolated from ion-exchange solution, which probably minimizes the amount of surface supported rhodium(0) nanoparticles and mainly yields rhodium(0) nanoparticles in the micropores of MIL-101. The rhodium loading of Rh/S-MIL-101 was found to be 1.95 % wt (corresponds to 0.18 mmol/g) by ICP-OES analysis. The drop in the amount of rhodium loading with respect to Rh@S-MIL-101 can be explained by the absence of surface supported rhodium(0) nanoparticles. In this context another control experiment was also performed by using unmodified MIL-101 and following the same procedure for the preparation of Rh/MIL-101. The rhodium loading of Rh/MIL-101 was determined to be 0.02 % wt by ICP-OES analysis, which supports our claim that this methodology followed in the preparation of Rh/S-MIL-101 mainly yields S-MIL-101 confined rhodium(0) nanoparticles not MIL-101 supported rhodium(0) nanoparticles. BFTEM image of Rh/S-MIL-101 is given in **Fig. 8(a)**, which showed that the majority of the rhodium(0) nanoparticles existed within the cavities of MIL-101 with an average

diameter of 1.95 ± 0.45 nm. The catalytic performance of Rh/S-MIL-101 in terms of activity and selectivity was tested in the hydrogenation of phenol under identical conditions (Rh concentration, phenol concentration, volume of H₂O and temperature) with those of Rh@S-MIL-101. We found that Rh/S-MIL-101 catalyst achieved the hydrogenation of phenol to cyclohexanone at 91 % conversion and 96 % selectivity at the end of 2 h with an initial TOF value of 70 mol cyclohexanone/mol Rh×h (Fig. 8(b)). This catalytic activity value is very close to that of obtained by Rh@S-MIL-101 so one can claim that rhodium (0) nanoparticles exist within the cavities of MIL-101 for Rh@S-MIL-101 catalyst play a major role in the hydrogenation of phenol to cyclohexanone.

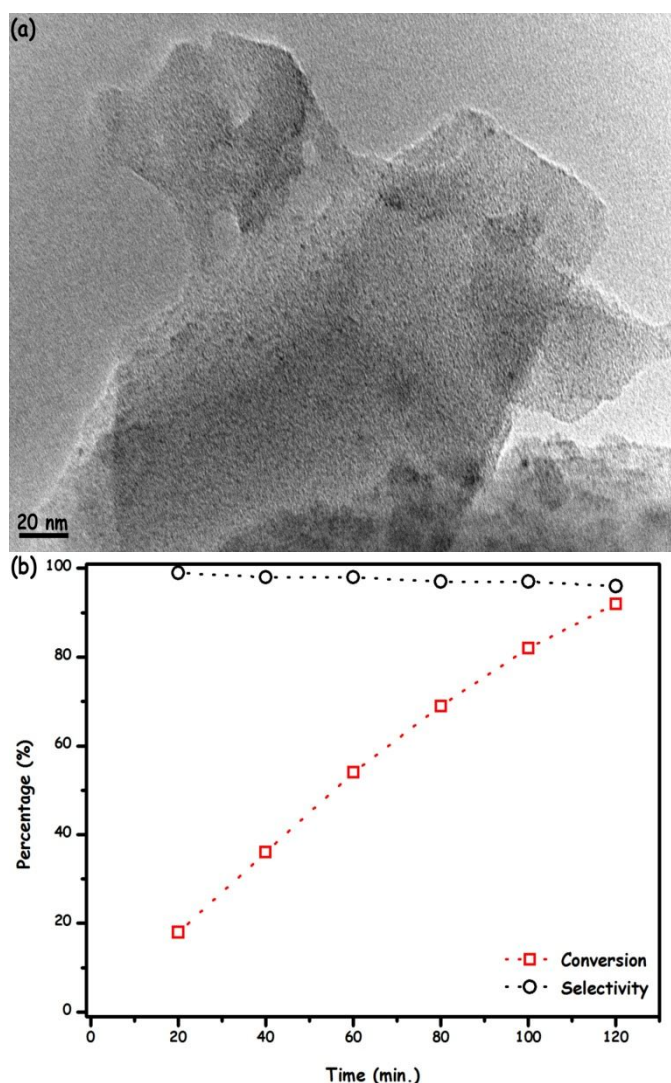
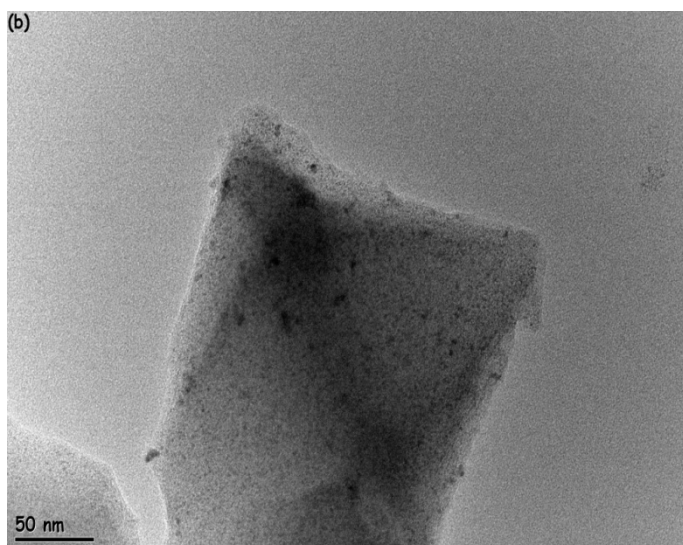
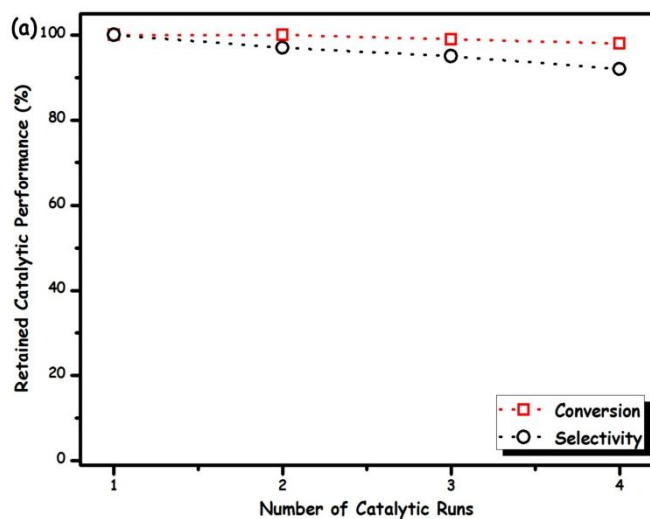


Fig. 8 (a) BFTEM image of Rh/S-MIL-101 and (b) The retained catalytic activity (%) and selectivity (%) for Rh/S-MIL-101 catalyzed hydrogenation of phenol.

The isolability, bottlability and reusability of Rh@S-MIL-101, as crucial measures in heterogeneous catalysis, were also tested in the hydrogenation of phenol. After 70 % conversion had been achieved, Rh@S-MIL-101 catalyst was isolated as powder form from the first catalytic run. The dried powder sample of Rh@S-MIL-101 can be bottled and stored under inert atmosphere.



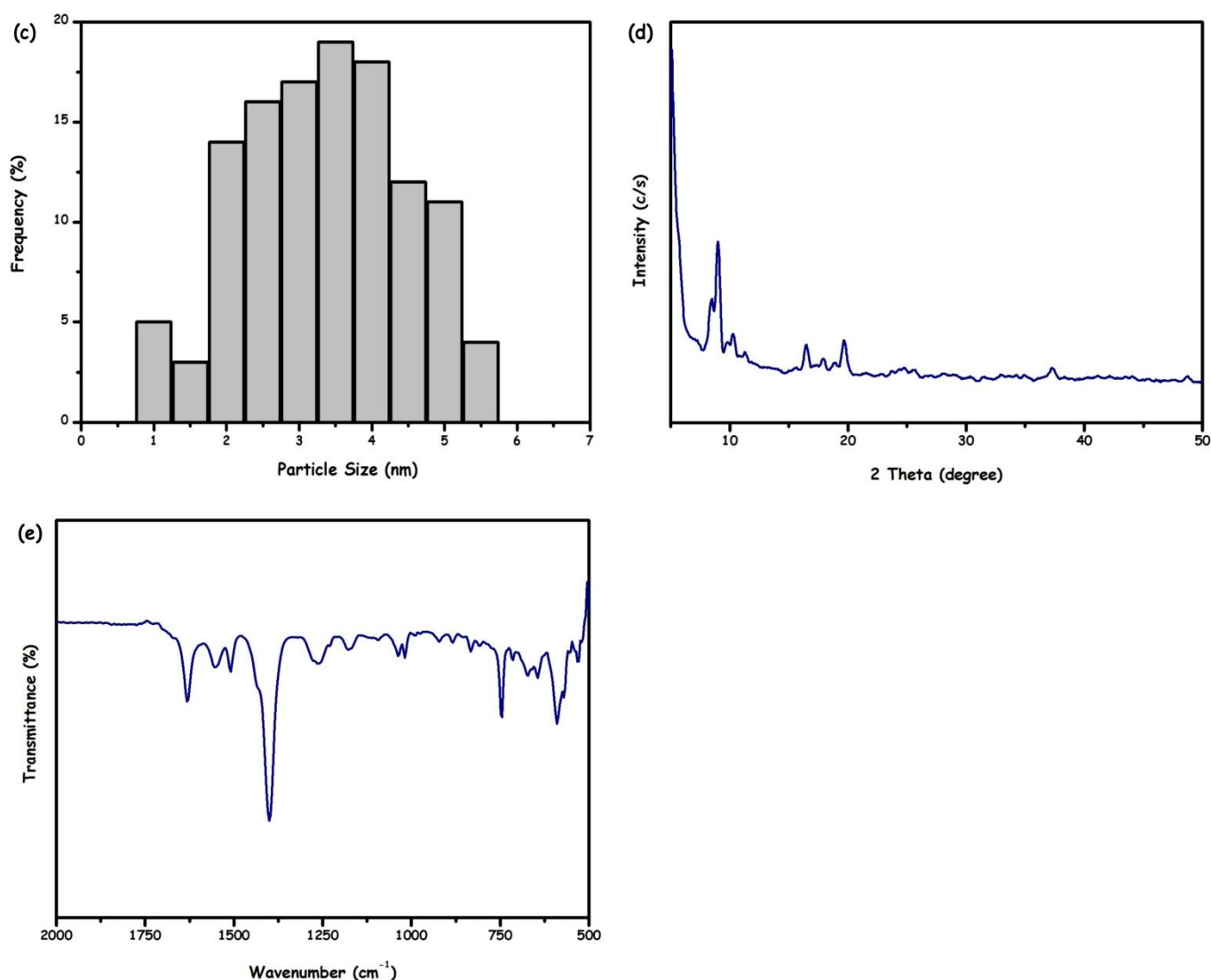


Fig. 9 (a) The percentage of retained catalytic activity and selectivity versus number of catalytic runs graph, (b) BFTEM image and corresponding size histogram (c), (d) P-XRD pattern and (e) FTIR spectrum of Rh@S-MIL-101 harvested after 4th catalytic reuse.

Furthermore, when Rh@S-MIL-101 was reused it was found to be still active catalyst in the selective hydrogenation of phenol to cyclohexanone, retaining > 98 % and > 92% of the initial catalytic activity and selectivity, respectively even at the fourth catalytic run (**Fig. 9(a)**). The slight decrease observed in the catalytic performance of Rh@S-MIL-101 can be attributed to a decrease in the number of active surface atoms due to an increase in the size of rhodium(0) nanoparticles from 2.35 ± 0.9 nm to 3.95 ± 0.95 nm (Figs. 9(b-c)). In the light of the previous studies [56-59], we believe that Ostwald ripening is an underlying process involved in Rh nanoparticles sintering, which involves the breaking of smaller Rh particle into a single-Rh atom fragment; $M_n \rightarrow M_1 + M_{n-1}$, followed by M_1 migration and agglomeration with a second larger sized particle M_m ; $M_1 + M_m \rightarrow M_{n-1} + M_{m+1}$ that yields larger, lower-surface area particles

that are typically less catalytically active. The final size of the resulting rhodium(0) nanoparticles are still smaller than the critical size regime ($d > 10$ nm) required for occurring of phase transition and Ostwald ripening only on the surface of catalyst [60]. Therefore, it is more acceptable to think that the Ostwald ripening of rhodium(0) nanoparticles (2.35 nm \rightarrow 3.95 nm) occurred not only on the surface of MIL-101 but also at the interface between the solid and liquid phases as a result of leaching/re-deposition. In addition to the sintering, the loss in the activity of rhodium(0) nanoparticles can also be attributed to an electron deficiency at the Rh sites. It has been shown elsewhere [61] that Rh particles > 3 nm have a tendency to remain electron deficient. There are many instances in the literature [1-3] where reactivity is strongly influenced by the electron density of supported metal nanoparticles. However, the results obtained from reusability experiments revealed that Rh@S-MIL-101 was isolable, bottleable, reusable active and selective heterogeneous catalyst for the hydrogenation of phenol to cyclohexanone. P-XRD analysis of the isolated sample from the fourth catalytic run (Fig. 9(d)) showed that the crystallinity of the host MIL-101 framework was retained. Additionally, FTIR spectrum of the recovered catalyst (Fig. 8(e)) is indicative of the existence of sulfonic acid groups in S-MIL-101 framework. More importantly, the filtrate solutions collected at the end of the each catalytic runs were analyzed by ICP-OES and in none of them Rh was detected, which confirmed the retention of rhodium within the MIL-101 matrix (no rhodium passed into the solution). A control experiment was also performed to show that the phenol hydrogenation was completely stopped by removal of Rh@S-MIL-101 from the reaction solution. Overall, these results are indicative of Rh@S-MIL-101 material is acting as highly active, selective, bottleable and reusable heterogeneous catalyst in the selective hydrogenation of phenol to cyclohexanone.

4. Conclusions

In summary, the main findings of this study plus their implications can be summarized as follows:

(i) Rh@S-MIL-101 catalyst was simply and reproducibly prepared, for the first time, by using a direct cationic exchange approach and subsequent reduction with sodium borohydride at room temperature. This synthesis protocol yields rhodium(0) nanoparticles (2.35 ± 0.9 nm) mainly located within S-MIL-101 by keeping the host framework intact, whereas the conventional reduction-deposition technique yields rhodium agglomerates in and on

unmodified MIL-101 framework. These results are indicative of the encapsulation and stabilization effect of sulfonate group on guest metal nanoparticles,

(ii) Testing the catalytic performance of Rh@S-MIL-101 in the selective hydrogenation of phenol to cyclohexanone in water under mild conditions (50 °C, 5 bar initial H₂ pressure) showed that Rh@S-MIL-101 acted as a highly active (lower limit of initial TOF = 78 mol cyclohexanone/mol Rh×h and true initial TOF value = 280 mol cyclohexanone/mol Rh×h by considering exposed surface Rh atoms) and selective (> 92 %) heterogeneous catalyst. The exceptional activity and selectivity of Rh@S-MIL-101 can be assigned to the combination of (1) host-guest cooperation between rhodium(0) nanoparticles and sulfonated MIL-101 framework and (2) the presence of Lewis acidic sites (Cr(III)) in MIL-101,

(iii) The catalytic stability of Rh@S-MIL-101 was investigated by performing reusability experiments in the phenol hydrogenation. Their results imply that Rh@S-MIL-101 is highly reusable (retains > 98 % activity and > 92 % selectivity even at 4th reuse) and durable heterogeneous catalyst for this reaction.

(iv) More importantly, Rh@S-MIL-101 catalyzed selective hydrogenation of phenol to cyclohexanone fulfilled the majority of the “green chemistry” requirements [62] including: (a) it used water as a solvent, (b) it was highly selective and prevents the formation of by-products; (c) it maximized the incorporation of reactant into the products; (d) it required mild conditions so it needed relatively low energy (50 °C with 5 bar initial H₂ pressure); (e) it was catalytic, not stoichiometric; (f) it did not use any protecting/deprotecting group; (g) real-time monitoring was easy by measuring the H₂ uptake or GC analysis.

Our study clearly showed that sulfonic acid functionalized MIL-101 acted as a good host material for the generation of small-sized catalytically active rhodium nanoparticles by preventing their agglomeration and leaching in the water mediated hydrogenation reaction. High activity, selectivity and reusability performance of Rh@S-MIL-101 catalyst make it very attractive catalyst for performing other selective hydrogenation reactions.

Acknowledgements

The financial support by the Scientific and Technological Research Council of Turkey (TUBITAK, Project No: 113Z307) is gratefully acknowledged.

References

-
- [1] M. Zahmakiran, S. Ozkar, *Nanoscale* 3 (2011) 3462.
- [2] D. Astruc, F. Lu and J. R. Aranzaes, *Angew. Chem. Int. Ed.* 44 (2005) 7852.
- [3] B. L. Cushing, L. Kolesnichenko, C. J. Connor, *Chem. Rev.* 104 (2004) 3893.
- [4] S. Özkar, R. G. Finke, *J. Am. Chem. Soc.* 124 (2002) 5796.
- [5] S. Özkar, R. G. Finke, *Langmuir* 19 (2003) 6247.
- [6] M. Zahmakiran, S. Özkar, *Langmuir* 24 (2008) 7065.
- [7] L. Tosheva, V. P. Valtchev, *Chem. Mater.* 17 (2005) 2494.
- [8] E. Castillejos, P. J. Debouttierre, L. Roiban, A. Solhy, V. Martinez, Y. Kihn, O. Ersen, K. Philippot, B. Chaudret, P. Serp, *Angew. Chem. Int. Ed.* 48 (2009) 2529.
- [9] M. Yurderi, A. Bulut, M. Zahmakiran, M. Kaya, *App. Catal. B: Env.* 160 (2014) 514.
- [10] M. Zahmakiran, Y. Tonbul, S. Özkar, *Chem. Commun.* 46 (2010) 4788.
- [11] M. Zahmakiran, Y. Roman-Leshkov, Y. Zhang, *Langmuir* 28 (2012) 60.
- [12] R. J. White, R. Luque, V. L. Budain, J. H. Clark, D. J. Macquarrie, *Chem. Soc. Rev.* 38 (2009) 481.
- [13] J. Y. Lee, O. K. Farha, J. Roberts, K. A. Scheidt, S. T. Nguyen, J. T. Hupp, *Chem. Soc. Rev.* 38 (2009) 1450.
- [14] A. Corma, H. Garcia, F. X. L. Xamena, *Chem. Rev.* 110 (2010) 4606.
- [15] A. Aijaz, Q. Xu, *J. Phy. Chem. Lett.* 5 (2014) 1400.
- [16] J. L. C. Rowsell, O. M. Yaghi, *Mic. Mes. Mater.* 73 (2004) 3.
- [17] G. Ferey, C. M. Draznieks, C. Serre, F. Millange, J. Dutour, S. Surble, I. Margiloski, *Science* 309 (2005) 2040.
- [18] A. Khutia, H. U. Remmelberg, T. Schmidt, S. Henninger, C. Janiak, *Chem. Mater.* 25 (2013) 790.
- [19] A. Aijaz, A. Karkambar, Y. J. Choi, N. Tsumori, E. Rönnebro, T. Autrey, H. Shioyama, Q. Xu, *J. Am. Chem. Soc.* 134 (2012) 13926.
- [20] Y. K. Hwang, D. Y. Hong, J. S. Chang, S. H. Jung, Y. K. Seo, J. Kim, A. Vimont, M. Daturi, C. Serre, G. Ferey, *Angew. Chem. Int. Ed.* 47 (2008) 4144.
- [21] Y. Huang, S. Liu, Z. Lin, W. Li, R. Cao, *J. Catal.* 202 (2012) 111.
- [22] M. S. El-Shall, V. Abdelsayed, A. E. Rahman, S. Khder, H. M. A. Hassan, H. M. El-Kaderi, T. E. Reich, *J. Mater. Chem.* 19 (2009) 7625.

-
- [23] Q. L. Zhu, J. Li, Q. Xu, *J. Am. Chem. Soc.* 135 (2013) 10210.
- [24] X. Gu, Z. H. Lu, H. L. Jiang, T. Akita, Q. Xu, *J. Am. Chem. Soc.* 133 (2011) 11822.
- [25] Y-Z. Chen, Y-X. Zhou, H. Wang, J. Lu, T. Uchida, Q. Xu, S-H. Yu, H-L. Jiang, *ACS Catal.* 5 (2015) 2062.
- [26] J. Hermannsdörfer, M. Friedrich, N. Miyajima, R. O. Albuquerque, S. Kümmel, R. Kempe, *Angew. Chem. Int. Ed.* 51 (2012) 11473.
- [27] Y. Zhang, J. Shi, F. Zhang, Y. Zhong, W. Zhu, *Catal. Sci. Technol.* 3 (2013) 2044.
- [28] J. S. Bradley, W. Busser, *Catal. Lett.* 63 (2009) 127.
- [29] L. Bromberg, Y. Diao, H. Wu, S. A. Speakman, T. A. Hatton, *Chem. Mater.* 24 (2012) 1664.
- [30] M. G. Goesten, J. J. Alcaniz, E. V. Ramos-Fernandez, K. Gupta, E. Stabitski, H. Van Bekum, J. Gascon, F. Kapteijn, *J. Catal.* 281 (2011) 177.
- [31] H. Liu, T. Jiang, B. Han, S. Liang, Y. Zhou, *Science* 326 (2009) 1250.
- [32] M. Zahmakiran, S. Özkar, *Mater. Lett.* 63 (2009) 1033.
- [33] M. Zahmakiran, S. Özkar, *J. Mater. Chem.* 19 (2009) 7112.
- [34] M. Annapurna, T. Parasuramulu, P. Vishnuvardhan, M. Suresh, P. R. Likhar, M. L. Kantam, *App. Org. Chem.* 29 (2015) 234.
- [35] B. Ostrowskagumkowska, J. Ostrowskaczubenko, *Eur. J. Polym.* 30 (1994) 869.
- [36] Y. Jin, J. Shi, F. Zhang, Y. Zhong, W. Zhu, *J. Mol. Catal. A:Chem.* 383 (2014) 167.
- [37] Z. Hasan, J. W. Jun, S. H. Jhung, *Chem. Eng. J.* 278 (2015) 265,
- [38] S. Storck, H. Bretinger, W. F. Maier, *Appl. Catal. A* 134 (1998) 137.
- [39] R. S. H. Mikhail, S. Brunauer, E. J. Bodor, *J. Colloid Interface Sci.* 26 (1968) 45.
- [40] F. Durap, M. Zahmakiran, S. Özkar, *Appl. Catal. A.* 369 (2009) 53.
- [41] X. Zhang, K.Y. Chan, *Chem. Mater.* 15 (2003) 451.
- [42] I. P. Jones, *Chemical Microanalysis Using Electron Beams*, The Institute of Materials, London, (1992).
- [43] S. Karahan, M. Zahmakiran, S. Ozkar, *Chem. Commun.* 48 (2012) 1180.
- [44] I. Dogson, K. Griffen, G. Barberis, F. Pignataro, G. Tauszik, *Chem. Ind.* 830 (1989) 1989.
- [45] C. V. Rode, U. D. Joshi, O. Sato, M. Shirai, *Chem. Commun.* (2003) 1960.
- [46] H. J. Wang, F. Y. Zhao, S. Fujita, M. Arai, *Catal. Commun.* 9 (2008) 362.
- [47] Y. Wang, J. Yao, H. Li, D. Su, M. Antonietti, *J. Am. Chem. Soc.* 133 (2011) 2362.
- [48] F. Lu, J. Liu, J. Xu, *Mater. Chem. Phys.* 108 (2008) 369.

-
- [49] J. He, C. Zhao, J. A. Lercher, *J. Catal.* 309 (2014) 362.
- [50] M. Zahmakiran, Y. Tonbul, S. Ozkar, *J. Am. Chem. Soc.* 132 (2010) 6541.
- [51] M. Zahmakiran, T. Kodaira, S. Ozkar, *App. Catal. B: Env.* 96 (2010) 533.
- [52] M. Zahmakiran, Y. R. Leshkov, Y. Zhang, *Langmuir* 28 (2012) 60.
- [53] M. Zahmakiran, S. Ozkar, *Inorg. Chem.* 48 (2009) 8955.
- [54] M. Zahmakiran, T. Ayvali, K. Philippot, *Langmuir* 28 (2012) 4908.
- [55] E. Bayram, R. G. Finke, *ACS Catal.* 2 (2012) 1967.
- [56] C. Aydin, J. Lu, A. J. Liang, C-Y. Chen, N. D. Browning, B. C. Gates, *Nano Lett.* 11 (2011) 5537.
- [57] J. Lu, C. Aydin, N. D. Browning, B. C. Gates, *J. Am. Chem. Soc.* 134 (2012) 5022.
- [58] A. Uzun, D. A. Dixon, B. C. Gates, *ChemCatChem* 3 (2011) 95107.
- [59] E. Bayram, J. Lu, C. Aydin, N. D. Browning, S. Ozkar, E. Finney, B. C. Gates, R. G. Finke, *ACS. Catal.* 5 (2015) 3514.
- [60] T. W. Hansen, A. T. Delariwa, S. R. Challa, A. K. Datye, *Acc. Chem. Res.* 46 (2013) 1720-1730.
- [61] J. J. Klink, *Lect. Not. Phys.* 684 (2006) 209.
- [62] M. Poliakoff, J. M. Fitzpatrick, T. R. Farren, P. T. Anastas, *Science* 297 (2002) 807.